



Three fission modes in ^{258}Md studied by Langevin model

Ishizaki Shoma^{†1}, Yoshihiro Aritomo¹, Mizuki Okubayashi¹, Katsuhisa Nishio², and Kentarou Hirose²

¹Faculty of Science and Engineering, Kindai University Higashi-Osaka, Osaka 577-8502, Japan

²Advanced Science Research Center, Japan Atomic Energy Agency Tokai, Ibaraki 319-1195, Japan

[†]Email: uthorium232@gmail.com

Recently, fission-fragment mass properties of ^{258}Md was measured in JAEA. The data indicates a mixture of fission modes. We tried to calculate the fission properties of ^{258}Md using the Langevin model.

1 Introduction

It has been shown that fission has multiple modes, characterized by mass asymmetric fission and mass symmetric fission [1-7]. In neutron-rich heavy element region, it is argued that several fission modes coexist, with a significant change of their yields in accordance with the number of neutrons contained in the fissioning nucleus. A typical example is found in the fermium isotopes. The dominant mode transition is from the asymmetric splitting for ^{257}Fm to the shape symmetric one for ^{258}Fm [8]. This transition was interpreted as due to the lowering of the fission barrier for symmetric fission toward heavier mass isotopes. It is important to know the potential energy surface structure and nuclear's deformation process to understand fission mechanism in neutron-rich heavy element region [9].

At the JAEA tandem facility, fission of an excited compound nucleus ^{258}Md was studied in the reaction of $^4\text{He}+^{254}\text{Es}$. Based on the systematics of the spontaneous fission [8], the nucleus are located in the region where mass-symmetric fission dominates.

For the discussion of the experimental data, we made a calculation of fission using the Langevin model. For the later discussion, we define three types of fission paths (modes); mass-asymmetric fission (standard mode), symmetric fission with high total kinetic energy TKE (supershort), and symmetric fission with low TKE (superlong).

2 Framework

We use the fluctuation-dissipation model and employ the Langevin equations[10] to investigate the fission process. The nuclear shape is defined by the two-center parametrization [11,12], which has three deformation parameters, z_0 , δ , and α to serve as collective coordinates: z_0 is the distance between two potential centers, α is a mass-asymmetry parameter defined by $(A_1 - A_2)/(A_1 + A_2)$ using fragment masses, A_1 and A_2 . The symbol δ denotes the deformation of the

fragments defined as $\delta = 3(R_{\parallel}R_{\perp})/(2R_{\parallel}+R_{\perp})$, where R_{\parallel} and R_{\perp} are the half length of the axes of an ellipse in the z_0 and ρ directions of the cylindrical coordinate, respectively, as shown in Figure 1 in Ref. [10].

We adopted the neck parameter $\varepsilon=0.55$ following the empirical relation in Ref. [9]. The three collective coordinates are abbreviated as q , $q = z, \delta, \alpha$. For a given value of a temperature of a system T , the potential energy is defined as a sum of the liquid-drop (LD) part, a rotational energy and a microscopic (SH) part:

$$V(q, l, T) = V_{LD}(q) + \frac{\hbar^2 l(l+1)}{2I(q)} + V_{SH}(q, T), \quad (1)$$

$$V_{LD}(q) = E_s(q) + E_c(q), \quad (2)$$

$$V_{SH}(q, T) = E_{shell}^0(q)\Phi(T), \quad (3)$$

$$\Phi(T) = \exp\left(-\frac{aT^2}{E_d}\right), \quad (4)$$

Here V_{LD} is the potential energy calculated with the finite-range liquid drop model, given as a sum of the surface energy E_S [12] and the Coulomb energy E_C . V_{SH} is the shell correction energy evaluated by the Strutinski method from the single-particle levels of the two-center shell model. The shell correction has a temperature dependence expressed by a factor $\Phi(T)$, in which E_d is the shell damping energy chosen to be 20 MeV [13] and a is the level density parameter. At the zero temperature ($T = 0$), the shell correction energy reduces to that of the two-center shell model values E_{shell}^0 . The second term on the right-hand side of Eq. (1) is the rotational energy for an angular momentum l [10], with a moment of inertia at q , $I(q)$.

The multidimensional Langevin equations [10] are given as

$$\frac{dq_i}{dt} = (m^{-1})_{ij} p_j, \quad (5)$$

$$\frac{dp_i}{dt} = -\frac{\partial V}{\partial q_i} - \frac{1}{2} \frac{\partial}{\partial q_i} (m^{-1})_{jk} p_j p_k - \gamma_{ij} (m^{-1})_{jk} p_k + g_{ij} R_j(t) \quad (6)$$

where $q = \{z, \delta, \alpha\}$ and $p_i = m_{ij} dq_j/dt$ is a momentum conjugate to coordinate q_i . The summation is performed over repeated indices. In the Langevin equation, m_{ij} and γ_{ij} are the shape-dependent collective inertia and the friction tensors, respectively. The wall-and-window one-body dissipation [14-16] is adopted for the friction tensor which can describe the pre-scission neutron multiplicities and total kinetic energy of fragments simultaneously [17]. A hydrodynamical inertia tensor is adopted with the Werner-Wheeler approximation for the velocity field [18]. The normalized random force $R_i(t)$ is assumed to be that of white noise, i.e., $R_i(t)=0$ and $R_i(t)R_j(t)=2\delta_{ij}\delta(t_1 - t_2)$. The strength of the random force g_{ij} is given by the Einstein relation $\gamma_{ij}T = \sum_k g_{ij}g_{jk}$

3 Results and discussion

Figure 1 shows the calculated results of the FFMDs and TKE distributions of ^{258}Md . FFMDs show mass symmetric splitting. The peak of the TKE distribution is about 235 MeV. From features, the short mode was dominant in the calculation results.

Figure 2 shows the evolution of each fission modes as a function of excitation energy of ^{258}Md (in this work, fission modes was defined in the range of mass numbers and TKE in Table 1). The calculation shows that the standard mode decreases with excitation energy. It is considered that this is because the shell structure responsible for mass-asymmetry decreases with excitation energy.

Figure 3 shows the fission pathways of each mode in the $z - \delta$ plane. From the 1st local minimum (around $\{z, \delta\} \sim \{0.0, 0.2\}$) to the 2nd local minimum (around $\{z, \delta\} \sim \{1.0, 0.2\}$), the three modes behave very similarly. But it can be seen that the standard mode branches first at $z \approx 1.3$ and then the superlong mode branches at $z \approx 1.8$.

Figure 4 shows the energy of the fissioning nucleus at each shape plotted as a function of z . In Figure 4, the saddle point is located at $z \approx 1.3$ in the standard mode, $z \approx 1.8$ in the superlong mode, and $z \approx 2.0$ in the supershort mode, so it was found that the branch point shown in Figure 3 is located at the saddle point. In particular, the saddle point of superlong mode is close to that of supershort mode, the trajectory is very similar up to the saddle point of superlong mode.

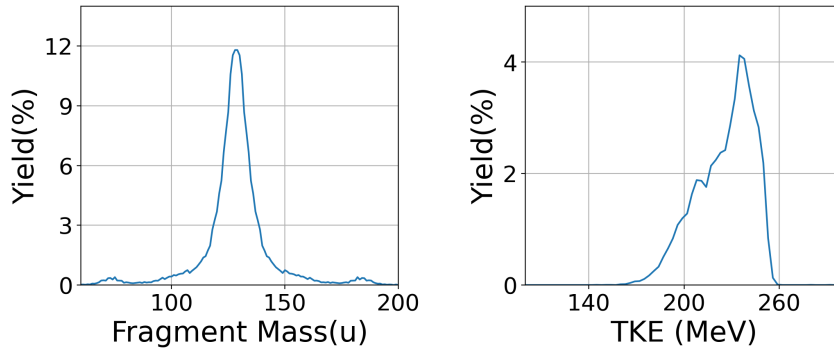


Figure 1: Calculation result of FFMDs (left) and TKE distribution (right) at excitation energy $E^* = 18 \text{ MeV}$

| mode | Mass | TKE |
|------------|----------------------------------------|-----------------------------------|
| supershort | $114 \leq \text{Mass} \leq 144$ | $\text{TKE} > 220 \text{ MeV}$ |
| superlong | $114 \leq \text{Mass} \leq 144$ | $\text{TKE} \leq 220 \text{ MeV}$ |
| standard | $114 > \text{Mass}, 144 < \text{Mass}$ | $\text{TKE} \leq 220 \text{ MeV}$ |

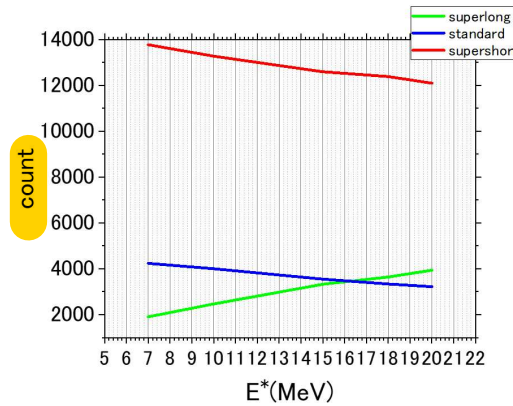


Figure 2: Each mode count as a function of excitation energy E^*

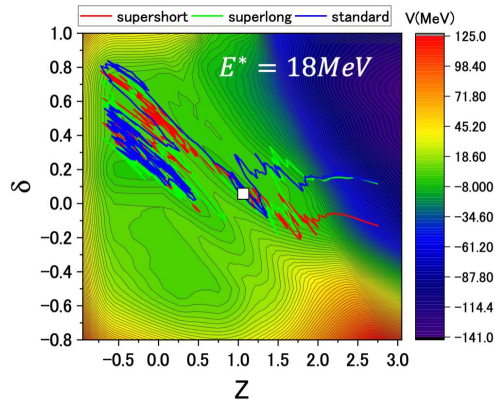


Figure 3: Each mode trajectory in $z - \delta$ plane on $\alpha = 0$ potential energy surface (The white square in the figure indicates the second minimum point)

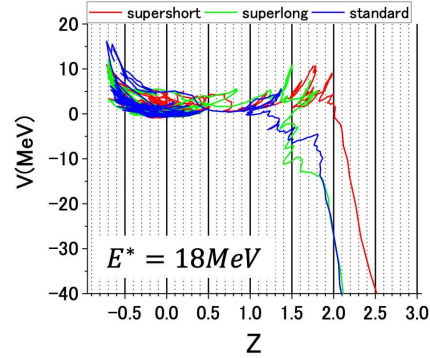


Figure 4: Each mode trajectory in $z - V$ plane

4 Conclusion

In this work, the fission mode of ^{258}Md was studied by trajectory calculation using a Langevin equations. As a result, it was found that each of the three modes bifurcate at the exit point of the 2nd local minimum on potential energy surface. Also, since supershort mode and superlong mode have very similar trajectory behavior up to the saddle point of superlong mode.

Acknowledgements

The Langevin calculations were performed using the cluster computer system (Kindai-VOSTOK) which is supported by Research funds for External Fund Introduction by Kindai University.

References

- [1] E. K. Hulet, J. F. Wild, R. J. Dougan, R. W. Loughheed, J. H. Landrum, A. D. Dougan,
- [2] P. A. Baisden, C. M. Henderson, R. J. Dupzyk, R. L. Hahn, M. Schdel, K. Smmerer, and G. R. Bethune, Phys. Rev. C 40, 770 (1989).
- [3] V. Pokrovsky, L. Calabretta, M. G. Itkis, et al., Phys. Rev. C 60, 041304
- [4] E. K. Hulet, R. W. Loughheed, J. H. Landrum, J. F. Wild, D. C. Hoffman, J. Weber, and J. B. Wilhelmy, Phys. Rev. C 21, 966 (1980).
- [5] J.F. Wild, J. van Aarle, W. Westmeier, R. Loughheed, E.K. Hulet, K.J. Moody, R.J. Dougan, E.-A. Koop, R.E. Glaser, R. Brandt and P. Patzelt, Phys. Rev., C 41, 640 (1990).
- [6] S. Cwiok P. Rozmej, A. Sobiczewski, and Z. Patyk, Nucl. Phys. A 491, 281 (1989).
- [7] U. Brosa, S. Grossmann, and A. Muller, Phys. Rep. 197,167 (1990).
- [8] D.C. Hoffman et al., Phys. Rev. C, 21, 1980 (637)
- [9] Y. Miyamoto et al., Phys. Rev. C, 99, 051601(R) (2019).
- [10] Y. Aritomo and M. Ohta, Nucl. Phys. A 744, 3 (2004).
- [11] K. Sato, A. Iwamoto, K. Harada, S. Yamaji, and S. Yoshida, Z. Phys. A 288, 383 (1978).
- [12] H. J. Krappe, J. R. Nix, and A. J. Sierk, Phys. Rev. C 20, 992(1979).

- [13] A. V. Ignatyuk, G. N. Smirenkin, and A. S. Tishin, *Sov. J. Nucl. Phys.* 21, 255 (1975).
- [14] J. Blocki, Y. Boneh, J. R. Nix, J. Randrup, M. Robel, A. J. Sierk, and W. J. Swiatecki, *Ann. Phys.* 113, 330 (1978).
- [15] J. R. Nix and A. J. Sierk, *Nucl. Phys. A* 428, 161c (1984).
- [16] H. Feldmeier, *Rep. Prog. Phys.* 50, 915 (1987).
- [17] T. Wada, Y. Abe, and N. Carjen, *Phys. Rev. Lett.* 70, 3538 (1993).
- [18] K. T. R. Davies, A. J. Sierk, and J. R. Nix, *Phys. Rev. C* 13, 2385 (1976).